^{63,65}Cu NMR and NQR evidence for an unusual spin dynamics in $PrCu_2$ below 100 K

A. Sacchetti,[1] M. Weller,[1] J. L. Gavilano,[2] R. Mudliar,[1,3] B. Pedrini,[1,4] K. Magishi,[1,5] H. R. Ott,[1] R. Monnier,[1] B. Delley,[6] and Y. Ōnuki[7]

[1]*Laboratorium für Festkörperphysik, ETH-Hönggerberg, CH-8093 Zürich, Switzerland*
[2]*Laboratory for Neutron Scattering, Paul Scherrer Institut, CH-5232 Villigen PSI, Switzerland*
[3]*Indian Institute of Technology, Bombay Powai, Mumbai 400076, India*
[4]*Institut für Molekularbiologie und Biophysik, ETH-Hönggerberg, CH-8093 Zürich, Switzerland*
[5]*Faculty of Integrated Arts and Sciences, The University of Tokushima, Tokushima 770-8502, Japan*
[6]*Paul Scherrer Institut, CH-5232 Villigen PSI, Switzerland*
[7]*Faculty of Science, Osaka University, Machikaneyama, Toyonaka, Osaka 560, Japan*

(Received 19 September 2007; published 2 April 2008)

We report the results of a ^{63,65}Cu NMR/NQR study probing the intermetallic compound $PrCu_2$. The previously claimed onset of magnetic order at 65 K, indicated in a muon spin resonance study, is not confirmed. Based on our data, we discuss different possible reasons for this apparent discrepancy, including a nonnegligible influence of the implanted muons on their environment. Competing dipolar and quadrupolar interactions lead to unusual features of the magnetic-ion/conduction-electron system, different from those of common intermetallics exhibiting structural or magnetic instabilities.

DOI: 10.1103/PhysRevB.77.144404 PACS number(s): 75.20.En, 71.70.Ej, 76.60.−k, 76.60.Es

I. INTRODUCTION

The Van Vleck paramagnet $PrCu_2$ exhibits peculiar electronic and magnetic properties, whose complete understanding is still to be achieved. The $4f$ electron ground-state multiplet of the Pr^{3+} ions is split into nine singlets by the crystal electric field. Nevertheless, an induced Jahn–Teller (JT) transition is observed at $T_{JT}=7.6$ K,[1,2] where the crystal structure changes from orthorhombic to slightly monoclinic.[3–5] An incommensurate antiferromagnetic (AF) order below $T_N=54$ mK among the Pr nuclear magnetic moments was claimed on the basis of magnetic susceptibility, specific heat, and neutron scattering measurements.[4,6] The respective moments align along the a direction of the orthorhombic unit cell with a propagation vector $\vec{q}=(0.24,0,0.68)$ in the reciprocal lattice. Magnetization and susceptibility measurements indicate a large polarization of the $4f$ Pr magnetic moments in the presence of an external field.[7,8] At low temperatures, the easy and hard magnetization axes are along the a and c directions, respectively. Quite surprisingly, the two magnetization axes are exchanged for fields exceeding 10 T, leading to a metamagnetic transition.[7,8] The $4f$ electron Pr-quadrupole moments play an important role in the physics of $PrCu_2$. In particular, the JT transition is ascribed to a phonon-mediated interaction between the quadrupole moments,[3] whereas the metamagnetic transition has been ascribed to a change in the orientation of the spatial charge distribution.[9]

Based on the results of a muon spin resonance (μSR) study, AF ordering of the localized Pr $4f$ electron moments below 65 K has recently been suggested.[10] Since such a magnetic transition in this temperature region is not reflected in the results of either neutron scattering or susceptibility experiments,[3,4,7] it may be assumed that the inferred magnetic order does not involve long-range order and static internal fields. Considering the electronic configuration of the Pr^{3+} ions, the above result is really unexpected and calls for additional checks. Since the μSR results may be due to dynamically induced nonvanishing internal fields, it is important to use a microscopic technique for investigating the phenomenon further. In this paper, we report a systematic study of $PrCu_2$ by means of Cu-based nuclear magnetic resonance (NMR) and nuclear quadrupole resonance (NQR) experiments between 4.2 K and room temperature.

II. EXPERIMENT

Nuclear resonance measurements were made using standard spin-echo techniques employing a phase-coherent pulsed spectrometer. ^{63,65}Cu NMR and NQR spectra were collected by measuring the integrated spin-echo signal as a function of the exciting radio frequency (rf) in fixed external magnetic fields. The spin-lattice relaxation rate (SLRR) T_1^{-1} was measured by destroying the z component of the equilibrium nuclear magnetization by means of a short rf pulse and monitoring its recovery as a function of a variable delay between this preparation pulse and a spin-echo sequence. The spin-spin relaxation rate (SSRR) T_2^{-1} was obtained from the τ dependence of the signal after a $\pi/2-\tau-\pi$ sequence.

Single-crystalline $PrCu_2$ samples were grown at Osaka University by means of the procedure described in Ref. 11. Since the system is metallic, the NMR signal from the single crystal is very small because the penetration depth of the rf pulses is of the order of 1 μm only. We observed an unexpected splitting and broadening of the NMR lines, which we traced back to a nonperfect orientation of the applied magnetic field with respect to one of the crystalline axes of the sample. From a detailed analysis, we concluded that meaningful NMR measurements on a single crystal of $PrCu_2$ require a precision in sample orientation that is much better than $\pm 1°$, which could not be achieved with our experimental setup. For this reason, we powdered the single-crystalline sample which not only served to avoid the orientation problem but also helped to enhance the NMR signal.

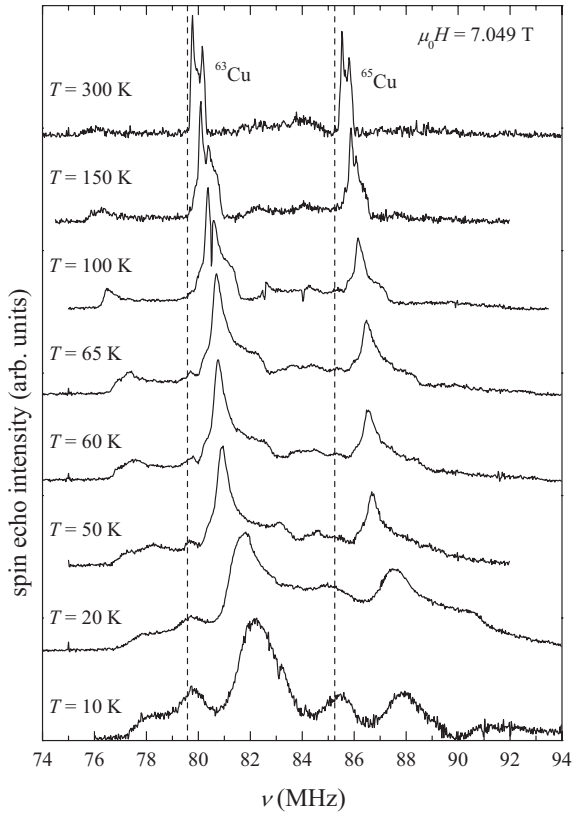

FIG. 1. ^{63,65}Cu NMR powder spectra of $PrCu_2$ at selected temperatures and in a field of 7.049 T. The vertical dashed lines mark the reference NMR frequencies for the two Cu isotopes (Ref. 12).

III. NMR MEASUREMENTS

Figure 1 shows the Cu NMR spectra of $PrCu_2$ powder at selected temperatures.

The 300 K spectrum is characterized by two main features centered at 80 and 86 MHz, which are ascribed to the NMR central lines of the ^{63}Cu and ^{65}Cu isotopes, respectively. Both isotopes possess a 3/2 nuclear spin but the gyromagnetic ratio of ^{65}Cu is roughly 7% larger than that of ^{63}Cu. We observe no sign of any contribution from the ^{141}Pr nuclei (reference frequency ~92 MHz at 7.049 T), most probably because their extremely large hyperfine coupling[6] produces a huge shift of the corresponding resonance and can result in very short relaxation times. Before we discuss all the Cu NMR spectra in detail, we note that all Cu sites are crystallographically equivalent and have an *m* point symmetry, i.e., they lie on a mirror plane perpendicular to the *a* axis. Both Cu NMR lines are split by ~1 MHz. We ascribe this splitting to a second-order quadrupolar perturbation of the Zeeman Hamiltonian. The wings observed between 75 and 90 MHz correspond to the first-order quadrupolar perturbation. These wings are more prominent at lower temperatures and it may be noted that, rather than a sharp edge, they exhibit a smooth edge suggesting, as explained below, a nonzero anisotropy η of the electric field gradient (EFG). With decreasing temperatures, the complexity of the spectrum increases. As can be seen in Fig. 1, the asymmetry and width of the lines grow and they partially merge together. The quadrupolar wings are strongly affected as well and a large overall shift of the lines toward higher frequencies is observed, indicating a progressively increasing Knight shift (K). The strongly asymmetric line shape suggests a large K anisotropy.

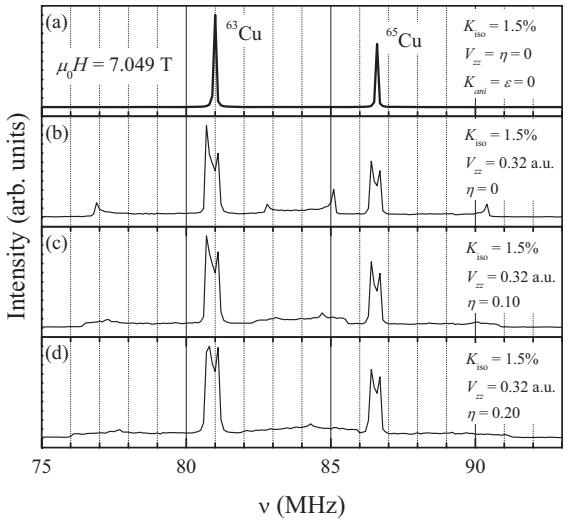

FIG. 2. Simulated ^{63,65}Cu NMR powder spectra in a field of 7.049 T with K_{iso}=1.5% and for different values of the EFG parameters (see text).

The very complex structure of the low temperature NMR spectra, caused by the simultaneous EFG and K anisotropies, makes a quantitative analysis of the spectra very difficult. Therefore, we keep the interpretation mostly at a qualitative level. To this end, we performed several simulations of the ^{63,65}Cu NMR powder spectrum for different values of the microscopic parameters characterizing K and EFG. The simulations involve a full diagonalization of the nuclear Hamiltonian comprising the sum of the quadrupolar and the Zeeman term corrected by K. The spectrum is then obtained from the calculated transition energies and intensities, averaged over random crystal orientations in order to simulate a powder spectrum. The microscopic parameters characterizing the quadrupolar Hamiltonian are the largest component V_{zz} of the EFG and the anisotropy η in the xy plane. The parameters describing K are the isotropic and anisotropic components K_{iso} and K_{ani}, respectively, as well as an axial-asymmetry term ϵ. The notation is standard and exemplified, for instance, in Ref. 13 (pp. 62–64). Figure 2(a) shows the simulated spectra that we obtained by considering only an isotropic K_{iso}=1.5% and no quadrupolar contribution. Naturally, this spectrum consists of only one line for each isotope, slightly shifted with respect to the reference frequency. Figure 2(b) was obtained by adding an EFG with V_{zz} =0.32 a.u. and η=0. It is clear that this term induces the appearance of the wing structures and a splitting of the central lines. The effect of adding a non-zero anisotropy η is demonstrated in Figs. 2(c) and 2(d), where the calculations with η=0.10 and η=0.20, respectively, are displayed. Upon enhancing η, the sharp edge of the wings is progressively smeared out, leading to a simulated spectrum with a shape resembling the experimental data at 300 K. The overall comparison of the experimental data with the simulations of Figs.

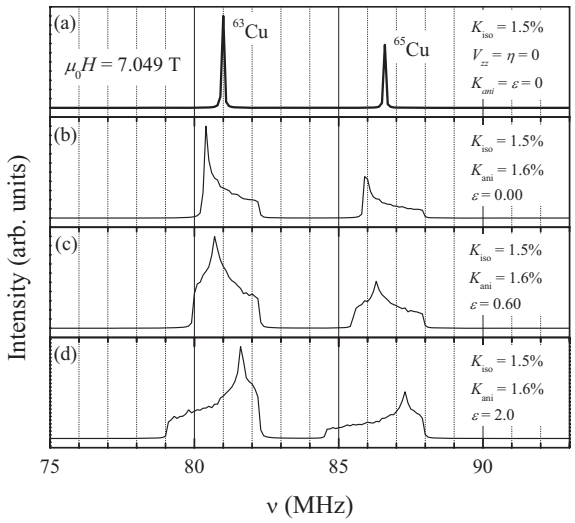

FIG. 3. Simulated powder ^{63,65}Cu NMR spectra at a field of 7.049 T and for different values of the K parameters (see text).

2(b)–2(d) suggests that the actual components of the EFG acting at the copper site in $PrCu_2$ are of the order of V_{zz} =0.32 a.u. and η=0.10, at least down to 100 K. An *ab initio* calculation in which the internal coordinates of the 12 ions in the unit cell of $PrCu_2$ were optimized assuming the experimental lattice parameters (a=4.4087 Å, b=7.0551 Å, and c =7.4441 Å)[5] using the DMOL^3 code[14] yielded V_{zz}=0.48 a.u. and η=0.11. Although the calculated absolute value of the EFG is 50% larger than that obtained by comparing experiment and simulations as described above, the direction of the dominant component of the EFG tensor is clearly established to lie in the bc plane. This is important for the discussion in Sec. V.

Figure 3(b) shows a simulated spectrum where the isotropic shift of 1.5% is augmented by an anisotropic component K_{ani}=1.6% but no axial asymmetry. The nonzero K_{ani} induces an asymmetric broadening of the central lines keeping rather sharp edges. The ϵ value is responsible for the position of the maximum with respect to the edges, as shown in Figs. 3(c) and 3(d), where the simulated spectra with ϵ=0.6 and ϵ=2.0 are shown, respectively.

Although these simulations allow for a qualitative description of the main features of the NMR spectra, the situation turns out to be much more complicated when we try to simultaneously take into account the influence of both EFG and K. These two contributions are indeed both nonnegligible and, in principle, temperature dependent. Moreover, the corresponding tensors are usually nondiagonal in the crystalline-axis frame and their main frames, i.e., the frames in which the two tensors are diagonal, are not necessarily oriented along the same directions. The local symmetry of the Cu sites provides one constraint for the EFG and K main frames. They should have one principal axis parallel to a. Concerning the orientation of the other two axes in the bc plane, nothing can be concluded from considering the crystal structure. Therefore, the angle between the K and EFG main frames in the plane is unknown. All the above considerations lead to the conclusion that the influences of both K and EFG on the spectral features cannot be regarded independently.

In spite of the difficulties described above, it is still possible to extract some quantitative information from the NMR spectra shown in Fig. 1. First of all, we can estimate the quadrupolar frequency ν_Q of ^{63}Cu from the widths of the wings. The data imply ν_Q=8–9 MHz with no significant change upon decreasing temperature, at least down to 50 K. Inserting V_{zz}=0.32 a.u. and η=0.10 into the relation

$$\nu_Q = \frac{3eV_{zz}Q}{2hI(2I-1)}\sqrt{1+\eta^2/3}, \tag{1}$$

where Q is the nuclear quadrupole moment and I is the nuclear spin, we obtain ν_Q=8.3±0.8 MHz. The second quantity that we can estimate is the largest principal component K_{max} of the K tensor. In the presence of a K anisotropy, the spectrum adopts the typical shape displayed in Figs. 3(b)–3(d).[13] The edges of the asymmetric broadening occur at frequencies $(1+K_{min})\nu_0$ and $(1+K_{max})\nu_0$, where K_{min} is the smallest component of the K tensor and ν_0 is the reference frequency of the considered nucleus.[13] The position of the resonance maximum is at $(1+K_{int})\nu_0$, where K_{int} is the third (intermediate) K-tensor main component.[13] The temperature dependence of the high-frequency edge can be followed down to ~20 K, thus allowing us to estimate $K_{max}(T)$.

We assume that the hyperfine field $\vec{B}^{hf}_{Cu}$ acting at the Cu site is mainly induced by the polarization of the Pr magnetic moments $\vec{\mu}_{Pr}$ via an interaction mediated by the conduction electrons, such that

$$\vec{B}^{hf}_{Cu} = \overleftrightarrow{A}\vec{\mu}_{Pr}, \tag{2}$$

where $\overleftrightarrow{A}$ is the tensor associated with the transferred hyperfine field. The orientation of one principal axis of the K tensor along the a axis and the fact that it represents the easy magnetization direction[7] indicate that the maximum K component most likely lies along a, as was also suggested by our preliminary measurements on the single crystal (data not shown here). The same is implied by our estimate of $K_{max}(T)$, which is found to be proportional to the susceptibility $\chi_a(T)$ along the a axis. For a given external magnetic field $\vec{B}_0$, $\vec{B}^{hf}_{Cu}$ and $\vec{\mu}_{Pr}$ can directly be obtained from K and the susceptibility, respectively. Using Eq. (2), we can calculate the diagonal term of $\overleftrightarrow{A}$ along a, namely,

$$A_{aa} = K_a(T)/\chi_a(T), \tag{3}$$

which is, of course, temperature independent and has a value of 0.54±0.02 T/μ_B. This value is very useful in the discussion of the NQR data.

A temperature-independent A_{aa} and the fact that we do not observe significant changes of the NMR spectrum around 65 K are not compatible with an ordering of the Pr moments at that temperature. Because of the interaction between the Pr moments and the conduction electrons, any incommensurate AF order of the Pr moments, as claimed in Ref. 10, is expected to have a strong influence on the Cu NMR response.

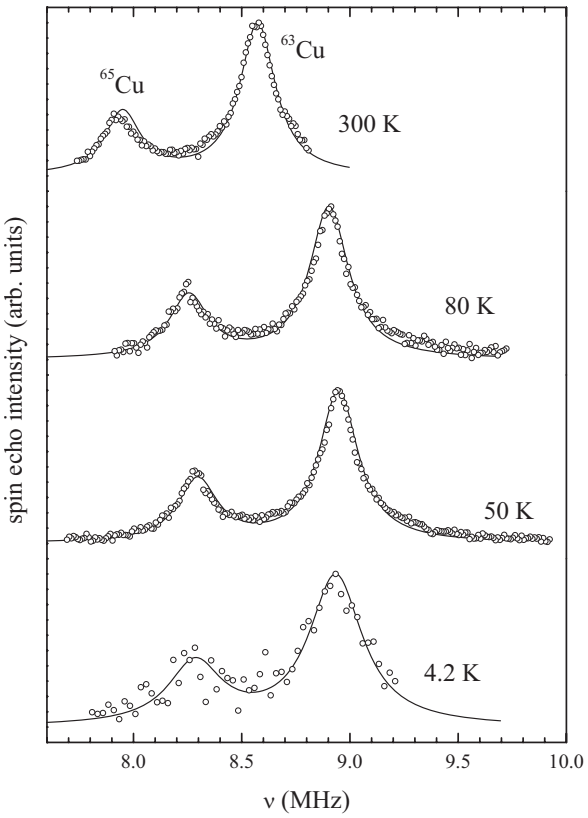

FIG. 4. ^{63,65}Cu NQR spectra of $PrCu_2$ at selected temperatures (symbols). Solid lines are best-fit curves to the data (see text).

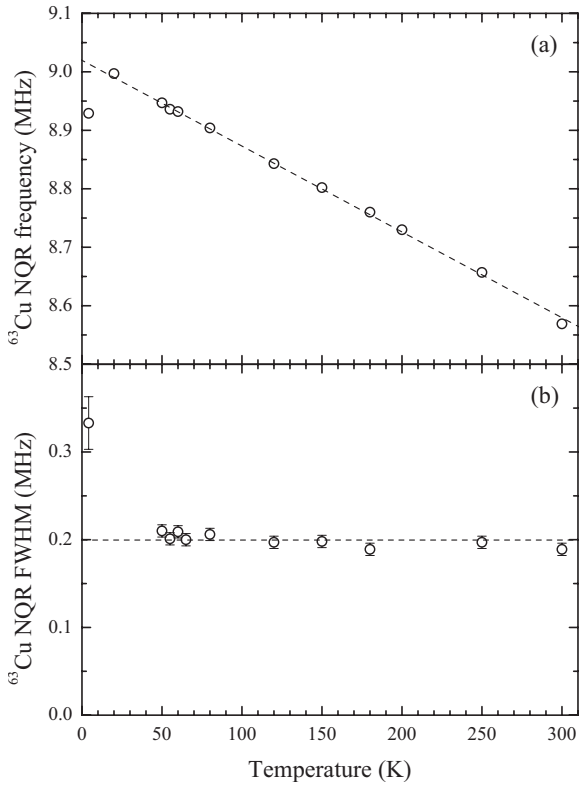

FIG. 5. Symbols: (a) ^{63}Cu NQR frequency and (b) linewidth of $PrCu_2$ as a function of temperature, as obtained from the best fits to the NQR spectra. The dashed lines represent (a) a linear fit and (b) the average of the data above 7 K.

IV. NQR MEASUREMENTS

A. Spectra

The rather large value of ν_Q indicated by the NMR data suggests that an NQR signal can be observed in an accessible frequency range. Figure 4 shows Cu NQR spectra at selected temperatures. The recorded data reflect the expected simple NQR spectrum with one single line per isotope, reflecting the respective $\pm 1/2 \rightarrow \pm 3/2$ transitions. The relative peak positions of the ^{63}Cu and ^{65}Cu signals are consistent with the nuclear quadrupole moment, which is roughly 8% larger for ^{63}Cu than for ^{65}Cu. From the raw data, it is clear that the ^{63}Cu NQR frequency is within 10% of the estimate of ν_Q obtained from the NMR spectra. The NQR frequency increases with decreasing temperature, whereas no major changes are observed in the T dependence of the linewidths. In order to obtain more quantitative information, we applied a best-fit procedure that is based on the frequency dependence of the intensity $S(\nu)$ given by

$$S(\nu) = \frac{A\alpha_{65}}{(\nu - \nu_Q/\beta)^2 + (\Gamma/2)^2} + \frac{A\alpha_{63}}{(\nu - \nu_Q)^2 + (\Gamma/2)^2}, \quad (4)$$

where A is the overall intensity, $\alpha_{65,63}$ are the natural abundances of ^{65,63}Cu, ν_Q is the ^{63}Cu NQR frequency, Γ is the linewidth (assumed to be equal for both isotopes), and $\beta = 1.078$ is the ratio between the quadrupolar moments of ^{63}Cu and ^{65}Cu. The experimental intensity $I(\nu, T)$ is

$$I(\nu, T) = S(\nu)\nu\left[1 - \exp\left(-\frac{h\nu}{k_B T}\right)\right], \quad (5)$$

where the multiplicative factor ν is due to the fact that our measurement is inductive; the term in square brackets represents the Boltzmann population factor. With this procedure, we fitted all the spectra using only A, ν_Q, and Γ as free parameters. Physically relevant are the latter two and we plot them as a function of temperature in Fig. 5.

The frequency ν_Q increases linearly with decreasing temperature down to T_{JT}, where a sudden drop in $\nu_Q(T)$ is observed. This reflects the JT structural transition which induces a sudden change in the EFG and thus in ν_Q. The overall change of ν_Q between 300 and 20 K is about 5%. Since ν_Q is related to both V_{zz} and η by means of Eq. (1), it is not possible to sort out whether the observed change in ν_Q is to be ascribed to V_{zz} or η, or both. Nevertheless, if we assume a constant V_{zz}, the $\nu_Q(T)$ values imply that the anisotropy should change from $\eta \sim 0.10$ at 300 K to approximately 0.60 at 20 K. Such a dramatic change in the asymmetry is very unlikely because it would require a strong modification of the electronic density, which does not seem to be compatible with the small anisotropy of the thermal expansion coefficients.[15] Moreover, no evidence of such a large variation can be inferred from the NMR data shown in Fig. 1 because in the presence of a large η, the edges of the quadrupolar wings are dramatically smeared out. It is therefore reasonable to ascribe most of the change in ν_Q to a

corresponding increase of V_{zz}, probably induced by the thermal contraction of the lattice.[15] The lack of any anomaly in $\nu_Q(T)$ around 65 K does not add support to the magnetic-order scenario inferred from the μSR data.

Between room temperature and T_{JT}, the linewidth Γ is almost constant. In particular, also $\Gamma(T)$ exhibits no anomaly around 65 K. Likewise, the absolute values of Γ are in contrast with a magnetic order of the Pr moments. Because of the interaction of the Pr moments with the conduction electrons, magnetic order among them would imply a local field $\vec{B}_{Cu}^{hf}$ acting on the Cu sites. As discussed above (Sec. III), the contribution to this field of any Pr moment oriented along a can be calculated by means of the corresponding hyperfine constant, i.e., $B_{Cu}^{hf}=A_{aa}\mu_{Pr}$. We calculated the local magnetic fields acting on Cu sites by invoking the six nearest-neighbor Pr moments, adopting the claimed AF configuration with an incommensurate modulation of the moments. The corresponding vector $\vec{q}=(0.24,0,0.68)$ and the modulation amplitude is $0.29\mu_B$.[10] We obtain a distribution of B_{Cu}^{hf} ranging from 0 to 0.06 T. Such a distribution of fields should be reflected in a broadening $\Delta\nu=1.4$ MHz of the NQR line. This value is almost 1 order of magnitude larger than Γ of our signals, thus indicating that a magnetic order of the claimed type[10] is incompatible with our data.

B. Relaxation

With the procedures described in Sec. II, we measured the time recovery of the longitudinal $m_L(t)$ and transversal $m_T(t)$ magnetizations. Representative examples of $m_L(t)$ and $m_T(t)$ are shown in the insets of Figs. 6(a) and 6(b), respectively. All the $m_L(t)$ curves can be fitted by means of the standard exponential function that applies for $I=3/2$,[16] namely,

$$m_L(t)=m_L(\infty)\left[1-\exp\left(-\frac{\rho t}{T_1}\right)\right], \tag{6}$$

where $m_L(\infty)$ is the equilibrium magnetization, T_1 is the spin-lattice relaxation time, and ρ is an η-dependent parameter, which can be approximated with $\rho\simeq 3$ for $0\lesssim\eta\lesssim 0.2$.[16] Because the standard dipole-dipole interaction is not the main spin-spin relaxation mechanism, $m_T(t)$ cannot be fitted by means of a simple exponential function. The stronger indirect interaction mediated by the conduction electrons via the Ruderman–Kittel–Kasuya–Yosida mechanism leads to a Gaussian correction[17,18] such that

$$m_T(t)=m_T(0)\exp\left[-\frac{t}{T_R}-\frac{1}{2}\left(\frac{t}{T_{2G}}\right)^2\right], \tag{7}$$

where $m_T(0)$ is the initial transverse magnetization, T_{2G} is the Gaussian spin-spin relaxation time, and $T_R=3T_1/(2+r)$ is a time scale depending on the SLRR and on its anisotropy r. Since this anisotropy is expected to be not as large as, e.g., in the layered copper oxides ($r\sim 4$), we assume $r\sim 1$ and hence $T_R\sim T_1$. As long as T_R is significantly larger than T_{2G}, their values are quite independent. Our assumption $T_R=T_1$ is thus justified *a posteriori*, both by the good quality of the fits and by the fact that we obtain systematically $T_{2G}<T_1$.

From the fits based on Eqs. (6) and (7), we obtain the temperature dependencies of the SLRR and SSRR, as shown in Figs. 6(a) and 6(b), respectively. Neither $T_1^{-1}(T)$ nor $T_{2G}^{-1}(T)$ exhibit the expected features that would reflect an onset of magnetic order around 65 K. The fluctuations that accompany such a transition should cause a distinct enhancement of the relaxation rates, resulting in a peak in $T_1^{-1}(T)$ around the ordering temperature. From Fig. 6(b), we take it that $T_{2G}^{-1}(T)$ is constant down to around 40 K where it starts to increase with decreasing temperature, displaying a peak at T_{JT}. The decrease of $T_{2G}^{-1}(T)$ below T_{JT} most likely reflects the reduction of the quadrupolar fluctuations. Also, $T_1^{-1}(T)$ peaks at T_{JT}, but the behavior at higher temperature is more difficult to interpret. The temperature dependence of the SLRR is neither compatible with a dominating relaxation via conduction electrons $[T_1^{-1}(T)\sim T]$ nor a relaxation via local magnetic moments (T_1^{-1}=const) or by spin-wave-type excitations ($T_1^{-1}\sim T^3$). Instead, $T_1^{-1}(T)$ exhibits a power-law-type behavior characterized by a negative exponent (−1.4) between 8 and 100 K and a positive one (0.4) above 100 K. In order to interpret this puzzling behavior, we tried to determine the leading spin-lattice relaxation mechanism by measuring T_1 also for ^{65}Cu. With $^{63,65}T_1$, $^{63,65}\gamma$, and $^{63,65}Q$, we denote the spin-lattice relaxation time, the gyromagnetic ratio, and the quadrupole moment of ^{63,65}Cu, respectively. If the dominant mechanism is magnetic,

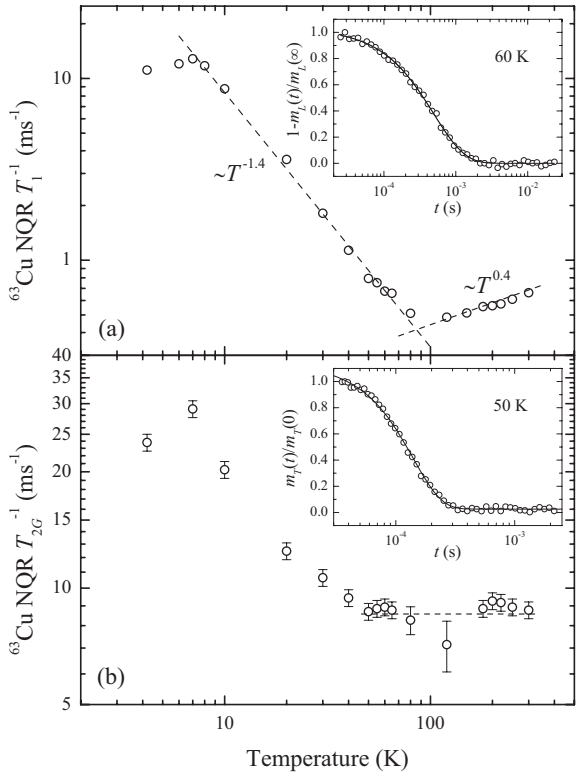

FIG. 6. (a) Spin-lattice and (b) spin-spin relaxation rates as a function of temperature. Dashed lines in (a) are power-law fits to the data in the temperature range above and below 100 K. The uncertainty of the data points in (a) is of the order of the diameter of the open circles. The horizontal dashed line in (b) is a guide to the eyes. Insets: examples of the time dependent (a) longitudinal and (b) transversal magnetizations. Solid lines in the insets of (a) and (b) are best fits to data according to Eqs. (6) and (7), respectively.

$$^{63}T_1/^{65}T_1 = (^{65}\gamma/^{63}\gamma)^2 = 1.167, \quad (8)$$

whereas for a relaxation driven by the quadrupolar interaction, we expect

$$^{63}T_1/^{65}T_1 = (^{65}Q/^{63}Q)^2 = 0.872. \quad (9)$$

We established that below 100 K, $^{63}T_1/^{65}T_1 \simeq 1.1$, which indicates that the relaxation is predominantly of magnetic origin. At higher temperature, we find $^{63}T_1/^{65}T_1 \simeq 1$, suggesting that the magnetic and quadrupolar interactions are of comparable importance. The fact that the magnetic fluctuations dominate below 100 K suggests that the internal field, if any is present, is not static. It is also worth mentioning that the puzzling $T_1^{-1}(T)$ cannot be ascribed to the temperature dependence of the population of the Pr levels in simple terms. Such a case would require that the lifetimes of these levels are different for each of them. Bearing in mind the single-exponential behavior exhibited by all our $m_L(t)$ curves, this possibility appears as rather unlikely.

V. COMPARISON BETWEEN NMR/NQR AND MUON SPIN RESONANCE MEASUREMENTS

Since the features extracted from the NQR data do not confirm but rather rule out AF ordering of the Pr moments at 65 K, it seems in order to discuss possible causes for this discrepancy. At present, we consider two possible explanations which may also apply in parallel. The first is based on the assumption that the observed order is not static but fluctuates on a time scale of the order of 1 μs. As a second possibility, we consider that the apparent order observed with muons is mainly due to a muon-induced local enhancement of slow spin fluctuations.

With μSR and the related precession frequency of the order of 10 MHz,[10] a nonzero field would be indicated. The characteristic time period in employing the NMR/NQR spin-echo technique is in the range of tens of microseconds. Therefore, the field fluctuations in the megahertz range would be averaged to zero and thus would not affect the resonance signal. Under these circumstances, μSR would indicate a "static" magnetic correlation with a distribution of internal fields, whereas the NMR/NQR spectra would not reflect such an effect.

Our *ab initio* calculations indicate that the dominant axis of the EFG and thus the quantization direction in NQR are orthogonal to the *a* axis (see Sec. III). If we assume that the internal field along *a* observed by μSR is not static but fluctuates, this would result in a large SLRR, whereas it should have only minor effects on the SSRR. This is consistent with our observation that on decreasing the temperature, $T_1^{-1}(T)$ increases much more rapidly than $T_{2G}^{-1}(T)$. As mentioned above, this scenario could reconcile the NMR/NQR data with the μSR results, provided that the time scale of the spin polarization is long ($\sim$1 μs). This would also be consistent with the observation of a Gaussian transverse relaxation since the presence of such a term requires an enhancement of the low-frequency components of the local susceptibility,[18] i.e., a slowing down of the spin dynamics.

In order to reconcile the results of the NMR/NQR and μSR experiments, we also consider the possibility that the magnetic order observed by μSR is mimicked by a quasistatic local enhancement of moment polarization by the probe itself. The muon, considered as a positive point charge, will attract electrons and thus lead to a rearrangement of charge and possibly of the ion positions. If, because of a slow enough spin fluctuation, the intrinsic electronic charge distribution is spin polarized during the duration of the muon lifetime, the muon will experience a spin density exceeding the one induced by the fluctuation. For our calculations,[19] we introduce a hydrogen atom[20] at the position of the muon derived by Schenck *et al.*[10] (1/2,1/4,0.6406) in every second cell along the *a* direction, which amounts to one muon per 8 f.u., and let all atoms relax at fixed volume. The resulting coordinates for the position of the muon are (1/2,1/4,0.6465), independent of the imposed spin polarization between 0 and $1\mu_B$ per unit cell. The Pr ions in the nearest-neighbor triangle are displaced, as shown in Fig. 7. The Pr-Pr distance is reduced by $\sim$0.3%, which corresponds to a compression by approximately 5 kbar.[21] At this point, it is worth mentioning that at external pressures exceeding 12 kbar, AF ordering of the Pr moments has been observed for $T \lesssim 9$ K,[21,22] thus indicating that a lattice compression enhances the magnetic correlations. Imposing a spin polarization of $1\mu_B$ per unit cell, which corresponds to an average spin density of 6.4×10^{-4} a.u., leads to a spin density at the muon site which is a factor of 6.6 larger than the average one. Reducing the imposed spin polarization by a factor of 4 yields a spin density at the muon 12 times larger than the average value. One might argue that the conclusions drawn from a calculation in which a hydrogen atom is placed in every second cell cannot be applied to the analysis of μSR experiments, which are performed with isolated muons. Our experience shows that if we double the number of hydrogens to one per cell, the enhancement of the spin density at the muon site is reduced by 15%. In other words, a larger dilution is expected to enhance the influence of the muon. So, there is no doubt that the presence of the muon affects the response of the system, namely, a small spin polarization in the system will be amplified at the muon site. A quantitative assessment of the temperature dependence of this extrinsic effect is out of reach of the presently used calculation method.

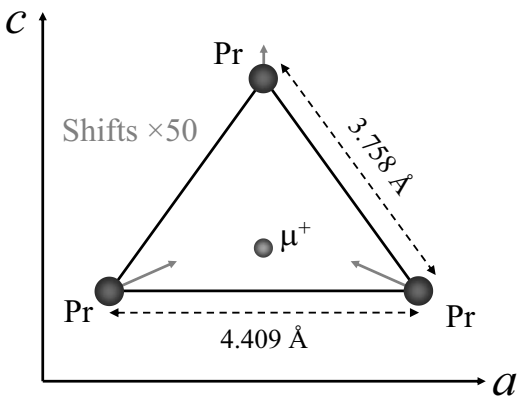

FIG. 7. Sketch of the positions of the Pr ions surrounding the muon, as obtained from the *ab initio* calculations (see text). The arrows indicate the displacement of the Pr ions (multiplied by 50) induced by the presence of the muon.

VI. CONCLUSIONS

The results of our NMR/NQR study of both the static (spectra) and dynamical (relaxation rates) microscopic magnetic properties of $PrCu_2$ provide no evidence for the onset of any magnetic order around 65 K that was previously claimed from μSR data.[10] As argued above, the μSR results may not reflect magnetic order but are rather due to a muon-induced local enhancement of slow polarization fluctuations. If the fluctuation has a time scale of the order of 1 μs, it could, as argued in Sec. V, appear as static in μSR and vanishing in NMR/NQR. The origin of the anomalous power-law behavior of the SLRR is not yet understood, but it clearly indicates that the magnetic behavior of $PrCu_2$ is far from that of a simple Pauli, Curie–Weiss type, or spin-wave system.

The present results call for further studies in order to clarify the complex magnetic properties of $PrCu_2$. In particular, it will be important to carry out NMR/NQR measurements in an AF phase. This could be obtained either by means of measurements below 54 mK or at pressures exceeding 12 kbar, where AF ordering among localized Pr moments has been observed for $T \lesssim 9$ K.[21,22]

ACKNOWLEDGMENTS

We thank A. Schenck for a detailed discussion of this work and we wish to acknowledge valuable contributions from J. Hinderer, S. Weyeneth, P. Wägli, E. Fischer, R. Helfenberger, H. R. Aeschbach, and F. N. Gygax. This research benefitted from financial support of the NCCR program MaNEP of the Schweizerische Nationalfonds für wissenschaftliche Forschung.

[1] M. Wun and N. E. Phillips, Phys. Lett. **50A**, 195 (1974).
[2] H. R. Ott, K. Andres, P. S. Wang, Y. H. Wong, and B. Lüthi, *Crystal Field Effects in Metals and Alloys: Induced Jahn-Teller Transition in* $PrCu_2$ (Plenum, New York, 1977).
[3] J. K. Kjems, H. R. Ott, S. M. Shapiro, and K. Andres, J. Phys. (Paris), Colloq. **6**, 1010 (1978).
[4] S. Kawarazaki and J. Arthur, J. Phys. Soc. Jpn. **57**, 1077 (1988).
[5] D. Scheptiakov and J. L. Gavilano (unpublished).
[6] K. Andres, E. Bucher, J. P. Maita, and A. S. Cooper, Phys. Rev. Lett. **28**, 1652 (1972).
[7] P. Ahmet, M. Abliz, R. Settai, K. Sugiyama, Y. Ōnuki, T. Takeuchi, K. Kindo, and S. Takayanagi, J. Phys. Soc. Jpn. **65**, 1077 (1996).
[8] R. Settai, M. Abliz, P. Ahmet, K. Motoki, N. Kimura, H. Ikezawa, T. Ebihara, H. Sugawara, K. Sugiyama, and Y. Ōnuki, J. Phys. Soc. Jpn. **64**, 383 (1995).
[9] R. Settai, S. Araki, P. Ahmet, M. Abliz, K. Sugiyama, Y. Ōnuki, T. Goto, H. Mitamura, T. Goto, and S. Takayanagi, J. Phys. Soc. Jpn. **67**, 636 (1998).
[10] A. Schenck, F. N. Gygax, and Y. Ōnuki, Phys. Rev. B **68**, 104422 (2003).
[11] M. Abliz, R. Settai, P. Ahmet, D. Aoki, K. Sugiyama, and Y. Ōnuki, Philos. Mag. B **75**, 443 (1997).
[12] R. K. Harris, E. D. Becker, S. M. Cabral De Menzes, R. Goodfellow, and P. Granger, Pure Appl. Chem. **73**, 1795 (2001).
[13] G. C. Carter, L. H. Bennett, and D. J. Kahan, *Metallic Shifts in NMR: A Review of the Theory and Comprehensive Critical Data Compilation of Metallic Materials* (Pergamon, New York, 1997).
[14] The calculations used the DNP basis set [B. Delley, J. Chem. Phys. **92**, 508 (1990); **113**, 7756 (2000)]. This basis set includes numerical atomic response functions of s, p, d (and f for Pr) character, in addition to the exact numerical solutions of the Kohn–Sham equations for each atom in the unit cell, and is expected to give better than 1 mhartree accuracy for the total energy per atom, in general. The basis functions have finite tails to help linear (in the number N of electrons) scaling methods. Only the density matrix had to be obtained by diagonalization, which is $O(N^3)$. Tail lengths were 8 a.u. in these calculations. The $\vec{k}$-space integrations have been performed with an unshifted $6\times4\times4$ mesh, which amounts to 36 symmetry-unique $\vec{k}$ points. A thermal broadening of 0.2 mhartree was used. The total energy has been modified with the entropy term proposed by M. Weinert and J. W. Davenport [Phys. Rev. B **45**, 13709 (1992)] to make the energy functional variational. Note that, in contrast to the total energy, the EFG is not a variational quantity with respect to the electronic density and therefore much more sensitive to small errors in the latter. All calculations were done for the orthorhombic structure and are therefore valid above the JT transition, which is where most of the experimental results have been obtained.
[15] T. Takeuchi, P. Ahmet, M. Anliz, R. Settai, and Y. Ōnuki, J. Phys. Soc. Jpn. **65**, 1404 (1996).
[16] J. Chepin and J. H. Ross, Jr., J. Phys.: Condens. Matter **3**, 8103 (1991).
[17] C. H. Pennington, D. J. Durand, C. P. Slichter, J. P. Rice, E. D. Bukowski, and D. M. Ginsberg, Phys. Rev. B **39**, 274 (1989).
[18] R. Stern, M. Mali, J. Roos, and D. Brinkmann, Phys. Rev. B **51**, 15478 (1995).
[19] In these calculations, the Pr $4f$ electrons were considered as part of the (rigid) ionic core, and the Pr valence electrons were described by a pseudopotential, since we were not interested in the density or spin density in the immediate neighborhood of the Pr nucleus.
[20] As far as static properties are concerned, a positive muon or a proton is equivalent. The choice of a neutral atom is justified by the efficient screening of the point charge by the surrounding electrons and avoids the introduction of an artificial neutralizing background in the total energy calculation. Nevertheless, we also performed a calculation in which the hydrogen atom is replaced by a positive point charge. The equilibrium position remains the same within 0.001 Å and the enhancement of the spin density is increased by 3%. Hence, our order of magnitude estimate of the effect should be valid, irrespective of the charge state of the introduced object representing the muon.
[21] T. Naka, J. Tang, J. Ye, A. Matsushita, T. Matsumoto, R. Settai, and Y. Ōnuki, J. Phys. Soc. Jpn. **72**, 1758 (2003).
[22] T. Naka, L. A. Ponomarenko, A. de Visser, A. Matsushita, R. Settai, and Y. Ōnuki, Phys. Rev. B **71**, 024408 (2005).